Optimized Power Dispatch in Wind Farms for Power Maximizing Considering Fatigue Loads

Baohua Zhang, *Student Member, IEEE*, Mohsen Soltani, *Senior Member, IEEE*, Weihao Hu, *Senior Member, IEEE*, Peng Hou, *Student Member, IEEE*, Qi Huang, *Senior Member, IEEE*, and Zhe Chen, *Senior Member, IEEE*

***Abstract*—Wake effects in a wind farm (WF) include the wind velocity deficit and the added turbulence. The wind velocity deficit may bring significant loss of the wind power and the added turbulence may cause extra fatigue load on the wind turbines (WTs). Inclusion of the wake effects in the wind farm control design can increase the total captured power by derating the upwind WTs. However, this may increase the turbulence and cause more fatigue load on the downwind WTs. This paper proposes an optimized active power dispatch strategy for WFs to maximize the total captured power while maintaining the fatigue load of the shafts and the towers within a certain range from the values using traditional strategy, which adopts maximum power point tracking (MPPT) control for each WT. A WT derating control strategy is included in the WT controller and the fatigue load for the tower and shaft is evaluated offline at a series of turbulence intensity, mean wind speed and active power reference to form a lookup table, which is used for the WF control. The proposed strategy is compared with WT MPPT control strategy and WF MPPT control strategy. The simulation results show the effectiveness of the proposed strategy.**

***Index Terms*—Active power dispatch, added turbulence, fatigue load reduction, power maximizing, wind farm.**

I. Introduction

NOWADAYS, wind power has become one of the most competitive renewable energy sources. Though the energy price for onshore wind is already the cheapest in some cases, the energy price of offshore wind is still higher than coal power plant and hydropower plant [1]. Meanwhile, the price decreasing of other renewable energies, like solar, brings threats to the wind industry. Therefore, reducing the cost of wind energy is a critical problem for wind industry.

Manuscript received December 3, 2016; revised April 24, 2017 and August 6, 2017; accepted August 31, 2017. Date of publication October 16, 2017; date of current version March 20, 2018. This work was supported by the National Natural Science Foundation of China under Grant 51707029. Paper no. TSTE-00947-2016. *(Corresponding author: Weihao Hu.)*

B. Zhang, M. Soltani, P. Hou, and Z. Chen are with the Department of Energy Technology, Aalborg University, Aalborg 9220, Denmark (e-mail: bzh@et.aau.dk; sms@et.aau.dk; pho@et.aau.dk; zch@et.aau.dk).

W. Hu is with the School of Energy Science and Engineering, University of Electronic Science and Technology of China, Chengdu 611731, China, and also with the Department of Energy Technology, Aalborg University, Aalborg 9220, Denmark (e-mail: whu@et.aau.dk).

Q. Huang is with the School of Energy Science and Engineering, University of Electronic Science and Technology of China, Chengdu 611731, China (e-mail: hwong@uestc.edu.cn).

Color versions of one or more of the figures in this paper are available online at http://ieeexplore.ieee.org.

Digital Object Identifier 10.1109/TSTE.2017.2763939

Reducing the cost by control is one of the emerging methods. Regarding to the wind farm level, the control focuses on maximizing the captured power and extending the lifetime by reducing the fatigue load [2].

Capturing more power can increase the benefit of WFs and fatigue load reduction will extend the lifetime of WTs, thus the cost of wind energy can be reduced. Both of these objectives are related to the control of the wakes, which represent the wind field changes when the wind passes WTs. The wakes may reduce the wind velocity at the downwind WTs and bring added wind turbulence, which will cause the loss of captured power and the increase of fatigue loads on the downwind WTs, respectively [3], [4]. Therefore, advanced WF control strategy is needed to reduce the wake effects, in order to capture more wind power and reduce the fatigue load.

There are two kinds of approaches for the wake control. The first is wake redirection approach, which redirect the wakes of the upwind WTs to avoid or minimize their effects to the downwind WTs. This approach can be achieved by pitching, yawing or independent pitch control [5]–[7]. The second approach is the axial induction factor based control, which adjusting the captured power of the upwind WTs to increase the total captured power in the WF [8]. This paper focuses on the axial induction factor based approach.

Usually, capturing more wind power and reducing the fatigue load cannot be achieved at the same time because adjusting power captured by the upwind WTs may bring higher wind turbulence to the downwind WTs and increase their fatigue load. Therefore, cooperative control should be developed to increase the captured power while considering the fatigue load.

Many research works tried to increase the captured power without considering the fatigue load [8]–[14]. These works focused on reducing the wake deficit by optimizing the axial induction factor of upwind WTs, which can improve overall wind power in the WF. The axial induction factor is directly selected as the control reference for each WT in [8] and [9]. This method only includes the wake deficit models into the optimization and is easy to be solved. However, setting the axial induction factor as the control reference of each WT needs modifications to the WT controller and may be very difficult to be implemented. The thrust coefficient which has a simple relation with the axial induction factor is selected as the control variable in [10], which also neglects WT control. The pitch angle was chosen as the optimization variable in [11] and [12], where the

WT aerodynamics are represented by a static WT model, and blade element momentum theory combined with eddy viscosity model, respectively. The pitch angle and the rotational speed are chosen as the optimization variables in [13]. Since the tip speed ratio and the rotational speed are simply related, the tip speed ratio together with the pitch angle are used in [14]. However, the normal control reference for a WT is the active power reference [15], with which the WT controller does not need modification. Therefore, it is better to set the active power reference of each WT as the control variables, then the rotational speed and the pitch angle can be determined by WT control strategies.

Beside focusing on the power maximization, another branch of works focus on minimizing the fatigue load of WTs [16]–[22]. However, two issues need to be addressed regarding this task, the first is how to find a representation of fatigue load that can be used for controller design, and the second is to find a way to evaluate the total effects of the fatigue load experienced by every WTs.

For the first issue, these are three kinds of solutions in literatures. The first solution is using average and standard deviations of thrust or movement to simply represent the fatigue load [17]–[21]. However, the standard deviation of the thrust cannot represent the effect of added turbulence to the fatigue [22]. The second solution is simply equal the wind turbulence to the fatigue load, i.e., to reduce the wind turbulence in order to mitigate the fatigue load [22], [23]. This method is interesting and may be better than the first one, however it is still an indirect way and will lead to inaccuracy. The third solution is adopting the Damage Equivalent Load (DEL) to represent the fatigue load. The DEL is defined as the amplitude of a sinusoidal stress of constant frequency that produces the same damage as the original signal in the same duration [17]. It is commonly used for evaluating the fatigue load [19]. However, it is usually used as a post evaluation index to test the control effects, rather than being directly used in the online control.

The second issue is how to evaluate the fatigue load at the WF level, i.e., how to find a way to evaluate the total effects of the fatigue load experienced by every WTs. Two ways to include the fatigue load at the WF level is proposed in [2]. One way is to minimize the sum of the WT fatigue load and another way is to minimize the maximal WT fatigue load. The first way can extend the sum of the lifetime of all WTs, while the second way can avoid the excessive lifetime reduction of one WT. From the WF owners' perspective, excessive lifetime reduction on one WT means they should replace this WT before other WTs reach their lifetime, which will cost more on installation, because renting the installation equipment is very expensive, especially for offshore WTs. Therefore, minimizing the maximal WT fatigue load may be better for reducing the total cost.

This paper proposes an optimized active power dispatch strategy for WFs to maximize the total captured power while maintaining the DEL of the shaft and the tower of each WT within a certain range from the values using traditional strategy. In order to introduce the fatigue load into optimization, the WT fatigue load is evaluated offline at a series of turbulence intensity, mean wind speed and active power reference to form a lookup table, which is used for the online optimization. The lookup table is generated by a WF simulator SimWindFarm, where the wind field is generated using Veers algorithm with Kaimal spectrum and WT is controlled with a WT derating control strategy. The simulation is performed for 600 mins totally at each operating point and the WT fatigue load is calculated by MCrunch code afterwards. The wind velocity inside the WF is calculated by Jensen model and the turbulence intensity is evaluated by a model proposed by Frandsen. The proposed strategy is compared with two traditional dispatch strategies in a designed WF and the optimization problems are solved by a modified particle swarm optimization algorithm.

The paper is organized as follows. Section II presents the WF farm model. Section III studies the traditional active power dispatch strategies and states the formulation of the proposed dispatch strategy. The effects of these strategies are compared and analyzed in Section IV. Finally, conclusions are brought in Section V.

II. Wind Farm Model

The WF model considered in this paper includes the WT model, WT fatigue load model, WF wind velocity model and the WF turbulence intensity model, which will be introduced separately in this paper.

A. Wind Turbine Model

The WT model used in this paper includes a static model based on lookup tables of the power coefficient and the thrust coefficient, a simple 3rd order drive train model, a 1st order generator model, 1st order pitch actuator, and a 2nd order tower dynamics [24].

The aerodynamics of the turbine can be described using three static relationships,

$$P_{\mathrm{mec}} = \frac{\pi}{2}\rho R^2 v^3 C_p\left(\beta,\lambda\right) \tag{1}$$

$$M_{\mathrm{shaft}} = \frac{\pi}{2}\rho R^2 v^3 C_p\left(\beta,\lambda\right)\Omega^{-1} \tag{2}$$

$$T_{\mathrm{tow}} = \frac{\pi}{2}\rho R^2 v^2 C_t\left(\beta,\lambda\right) \tag{3}$$

where P_{mec} is the WT mechanical power, M_{shaft} is the main shaft torque, T_{tow} is the tower thrust, C_p and C_t are two look-up tables derived with input tip speed ratio λ and pitch angle β, ρ is the air density, R is the rotor radius, v is the effective wind speed over the rotor, and Ω is the rotor rotational speed. The models of other parts of the WT can be found in [24].

The control strategy for the WT includes the control strategy under normal operation and control strategy under derating operation. The normal WT control strategy in the whole wind speed region can be divided into five regions [25]. In Region 1, the wind speed is below the cut-in wind speed and the WT does not produce power. In Region 2, the WT chases the maximum C_p by adjusting the rotational speed. In Region 3, the wind speed is above the rated wind speed and the WT keeps the captured power at the rated value by adjusting the pitch angle. In transition regions 1½ and 2½, the rotational speed is kept constant at the lower limit and the higher limit respectively.

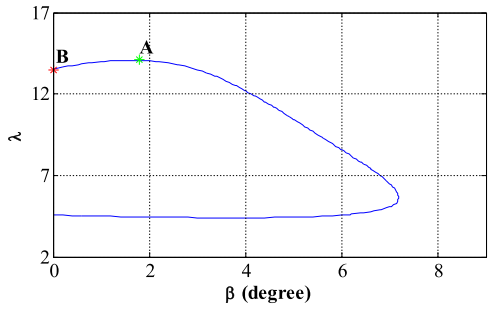

Fig. 1. The power coefficient level curve for the value of 0.3.

The derating control strategy is a modification from the normal control strategy, where the target in Region 2 is not always maximum power capturing, but keeping the captured power at the reference power in derated state. Fig. 1 shows the power coefficient level curve when C_P is 0.3. It can be observed that there are many options for choosing β and λ. In Region 2, the rotational speed ω can be changed between its lower and upper limits, which gives a wide range of λ.

The WT derating control strategy should be carefully designed because improper design may bring more load and increase the chance for the WTs operating in the stall region [26]. The Max-Ω control strategy for WT derating control proposed in [27] maximizes the rotational speed for each wind speed under each demanded power. The operating point A in Fig. 1 corresponds to the Max-Ω strategy. It can mitigate the load, decrease the chance of operating in stall region and bring more rotational energy in the rotor. In this paper, the derating strategy is similar to the Max-Ω strategy. The principle is using torque control firstly to regulate the captured power in the derating status, which will increase the rotational speed. Then, pitch control takes over if the rotational speed has reached its limits. The operating point B in Fig. 1 corresponds to the derating strategy used in this paper.

B. WT Fatigue Load Representation

The fatigue load of the shaft and the tower of a WT is evaluated by DEL in this paper. The DEL is calculated using Miner's rule [16], which depends on material properties specified by the slope of the S-N curve [17]. The DEL calculation is performed by MCrunch code (refers to [28]), with the S-N slope specified as 10 at the beginning of each channel.

The online evaluation of the fatigue load using DEL is still too time-consuming for the optimization in the WF controller, therefore an offline evaluation of the fatigue load is proposed in [29], which is also adopted in this paper. If the WT control strategy is determined, the fatigue load of the shaft and the tower can be affected by the turbulence intensity, the effective wind speed and the control reference from the WF controller, which is normally the active power demand of the WT $P_{\mathrm{ref}}^{\mathrm{WT}}$. Therefore, the fatigue load of the shaft and the tower can be evaluated offline at different combinations of turbulence intensity Ti, mean wind speed v and active power reference $P_{\mathrm{ref}}^{\mathrm{WT}}$.

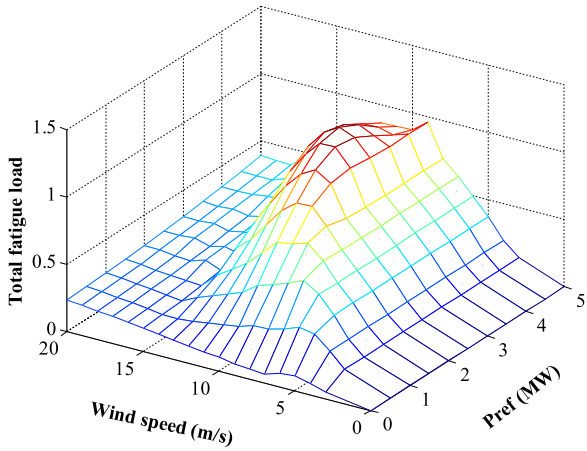

Fig. 2. The WT total fatigue load as change of wind speed and power reference when *Ti* is 0.1.

Then, the DELs of a the shaft and the tower can form two lookup tables $F_{\mathrm{shaft}}(Ti, v, P_{\mathrm{ref}}^{\mathrm{WT}})$ and $F_{\mathrm{tow}}(Ti, v, P_{\mathrm{ref}}^{\mathrm{WT}})$, and the total DEL of the WT F_{WT} can be defined as the combined effects of F_{shaft} and F_{tow} with the following equation:

$$F_{\mathrm{WT}} = K_{\mathrm{tow}} F_{\mathrm{tow}} + K_{\mathrm{shaft}} F_{\mathrm{shaft}} \tag{4}$$

where K_{tow} and K_{shaft} are the tunable weightings and can be tuned according to the costs and the designed lifetime of the shaft and the tower. Therefore, the total WT DEL can be searched from the lookup table $F_{\mathrm{WT}}(Ti, v, P_{\mathrm{ref}}^{\mathrm{WT}})$, which is very suitable for the optimization in the WF controller.

The lookup tables are generated by a wind farm simulation toolbox SimWindFarm, where the wind field is generated using Veers algorithm (refers to [30]) with Kaimal spectrum according to the recommendations in IEC 61400-3 concerning offshore turbines [24]. The WT model and WT control strategy are the same as introduced in sector A. The DEL calculation is performed by MCrunch code. As the wind field is generated stochastically, it is natural to implement the simulation for a long time at each operating point. The simulation is performed 600 mins in this paper, 10 mins each time, 60 times. The DEL of the shaft F_{shaft} and the DEL of the tower F_{tow} in 10 mins are transferred to per unit value separately, where the base values are the maximal DEL of the shaft and the maximal DEL of the tower separately. Then the lookup table of the total WT DEL is calculated using (4), where K_{tow} is chosen as one and K_{shaft} is chosen as two, based on the fact that the shaft is more vulnerable than the tower.

The WT total fatigue load $F_{\mathrm{WT}}(Ti, v, P_{\mathrm{ref}}^{\mathrm{WT}})$ at four different turbulence intensity are shown in Figs. 2–5. It can be seen that the total fatigue load in the high wind speed region is small when *Ti* is low, and it increases as *Ti* increases. This can be explained by the combined effects of the trend of the shaft fatigue load and the trend of the tower fatigue load, with the change of wind speed and power reference. As the wind speed and power reference increase, the fatigue load of the shaft increases in the region where the torque controller is responsible for regulating the power, whereas the fatigue load of the shaft decreases in the region where the pitch controller is dominant. This is easy to

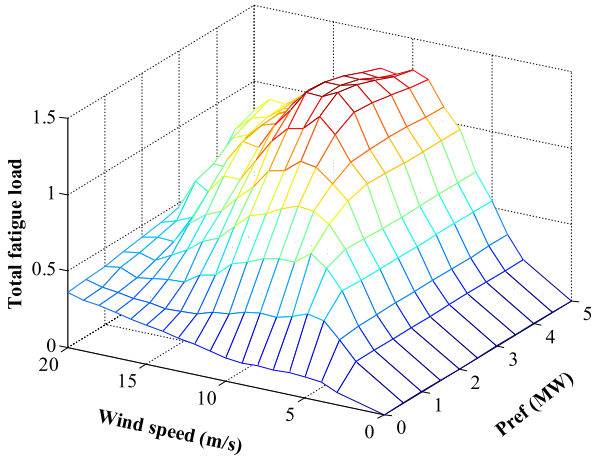

Fig. 3. The WT total fatigue load as change of wind speed and power reference when *Ti* is 0.2.

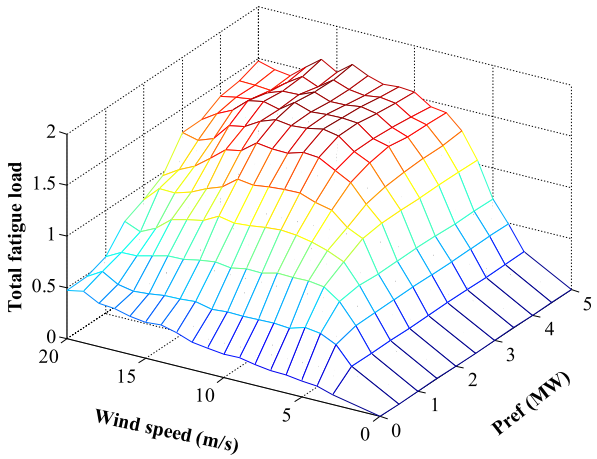

Fig. 4. The WT total fatigue load as change of wind speed and power reference when *Ti* is 0.3.

understand that when pitch controller is dominant, the load variation is mainly taken by the blade, which will mitigate the load variance on the shaft. The tower fatigue load is mainly caused by the change of the tower thrust T_{tow}, which is related to the wind speed, the pitch angle and the tip-speed ratio, as shown in (3). The trend of the tower fatigue load with the increase of wind speed and power reference can be found in [29]. As the total fatigue load is the combination of shaft fatigue load and tower fatigue load, it decreases in the high wind speed region when *Ti* is small. However, when *Ti* is high, the real time wind speed changes very significantly, which causes frequent transition between the torque control region and the pitch control region and brings more fatigue load on the shaft and the tower. This is the reason that the total fatigue load increases significantly in high wind speed region as *Ti* increases.

C. WF Wind Velocity Model

In the wake of an upwind WT, the average wind velocity decreases, which will cause the wind velocity deficit at the

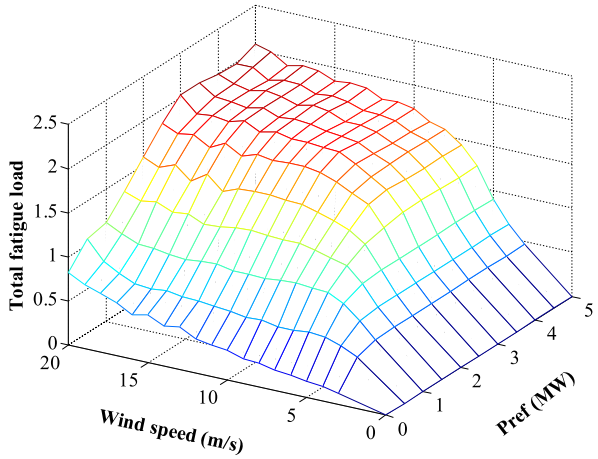

Fig. 5. The WT total fatigue load as change of wind speed and power reference when *Ti* is 0.4.

downwind WTs. The wind velocity on the downwind WTs is evaluated by the multiple-wake model, which is explained in [31]. Based on this model, the wind velocity at the WT *i* can be calculated by:

$$v_i = v_0 \cdot \left[1 - \sqrt{\sum_{j=1}^{N} \left[1 - \left(\frac{v_{j,i}}{v_0}\right)\right]^2}\right] \tag{5}$$

where *N* is the number of wakes, v_0 is the ambient wind speed, $v_{j,i}$ is the wind velocity deficit at WT *i* produced by the wake *j*, which is simulated by Jensen wake model [3], [32]:

$$v_{j,i} = v_0 - v_0 \cdot \left(1 - \sqrt{1 - C_{t,j}}\right) \cdot \left(\frac{R_i}{R_{j,i}}\right)^2 \cdot \left(\frac{S_{\mathrm{overlap},j}}{S_i}\right) \tag{6}$$

$$R_{j,i} = R_j + k \cdot L_{j,i} \tag{7}$$

where $C_{t,j}$ is the thrust coefficient of the wake-generating WT *j*, R_i is the rotor radius of WT *i*, $R_{j,i}$ is the radius of wake *j* at the distance $L_{j,i}$, S_i is the rotor area of WT *i*, $S_{\mathrm{overlap},j}$ is the overlap area of wake *j* and WT *i*, and *k* is wake decay constant, which is recommended as 0.04 for offshore WF [33].

D. WF Turbulence Intensity Model

The wakes in a WF can not only cause wind velocity deficit at downwind WTs, but also increase the turbulence intensity at WTs in the wake region. The increase in the turbulence intensity is evaluated by the added turbulence intensity, which can be calculated by the method proposed by Frandsen [34]:

$$I_{\mathrm{add},j} = \frac{1}{1.5 + 0.8 s_j / \sqrt{C_{T,j}}} \tag{8}$$

where $s_j = x/D_0$ is the dimensionless distance from the wake-generating WT *j* to the wake-effected WT, *x* is the distance between wake-generating and wake affected WT, D_0 is the rotor diameter.

For a WT in a large WF, where the downwind WT is exposed to wakes from several upwind WTs, this one-wake model needs to be extended to multiple-wake model, which is also given by Frandsen [34]:

$$I_i(\theta) = I_0(\theta)\left(1 + \sum_{j=1}^{N} \alpha_j \exp\left(-\left[\frac{\theta - \theta_j}{\theta_{w,j}}\right]^2\right)\right) \tag{9}$$

where θ is the wind direction, I_0 is the turbulence intensity of the ambient wind field, θ_j is the corresponding azimuth direction of wake no. *j*, $\theta_{w,j}$ is the a characteristic view-angle of the wake-generating WT *j* seen from the wake-effected WT, and α_j can be calculated by

$$\alpha_j = \sqrt{\left(\frac{I_{\mathrm{add},j}}{I_0}\right)^2 + 1} - 1. \tag{10}$$

III. Active Power Dispatch Strategies

This section introduces the traditional WF control strategy and the active power dispatch strategy for the WF Maximum Power Point Tracking (MPPT), and proposes a new active power dispatch strategy that can maximize the captured power of the WF while maintaining the DEL of the shaft and the tower of each WT within a certain range from the values using traditional strategy.

A. Strategy A: MPPT for Each WT

This is the traditional active power control strategy of the WF. This strategy is used when the system operation has no power constraint to WF or the WF operator ignore the power constraint. In this case, the WT output power has no constraint, thus the WT is controlled using its control strategy under normal operation, which has been discussed in Section II-A. The WT strategy tracks the maximum power coefficient $C_p^{\max}$ of each WT when the effective wind speed is under the rated wind speed, however it will cause more wake effects to the downwind WTs [35].

B. Strategy B: MPPT for the WF

This strategy maximizes the captured power of the WF by adjusting C_p and C_t of each WT at the same time. It reduces the captured power at the upwind WTs in order to reduce the wind velocity deficit at downwind WTs, thus to increase the total captured power in the WF. This strategy needs a centralized controller to coordinate each WT.

There are many ways to design the outputs of the WF controller, which are also the inputs of the WTs. Many of the reviewed papers took the axial induction factor, the thrust coefficient, the pitch angle, the rotational speed (tip speed ratio), or the combination of two of them as the inputs of the WTs. However, the outputs of the WF controller are usually the power reference of each WT. Therefore, it is better to use the power reference of each WT as the control variable of the WF controller, and the other variables as the dependent variables. This control variable has been adopted in [29], [36], [37].

The objective function of the problem can be expressed as:

$$\max_{P_{\mathrm{ref}}^i} \quad \sum_{i=1}^{N} P_{\mathrm{mec}}^i \tag{11}$$

$$0 \le P_{\mathrm{ref}}^i \le P_{\mathrm{WT}}^{\max} \tag{12}$$

where P_{mec}^i is the captured power by WT i, N is the number of WTs, and P_{ref}^i is the reference power to WT i. The control variable P_{ref}^i should remain within zero and the rated power.

C. Strategy C: The Proposed Strategy

The strategy B can increase the captured power in the WF, however it may also cause more fatigue load on the WTs. Therefore, Strategy C is proposed in this paper to raise the capture power while maintain the fatigue load level of the WF within a certain range from the values using traditional strategy. The fatigue load level of the WF is defined as the maximum fatigue load experienced by every WTs inside the WF, and the WT fatigue load is the combination of the shaft fatigue load and the tower fatigue load, as in (4). The advantage of using this criterion to represent the total fatigue load effects of all the WTs is that it can avoid excessive fatigue load on one WT, which can ensure the WTs reach their lives closely to reduce the replacement cost. The fatigue load level of the WF can be calculated using the following equation:

$$F_{\mathrm{WF}} = \max_i F_{\mathrm{WT}_i} \tag{13}$$

where F_{WF} is the fatigue load level of the WF and F_{WT_i} is the fatigue load of WT *i*.

The optimization problem of this strategy can be expressed as:

$$\max_{P_{\mathrm{ref}}^i} \quad \sum_{i=1}^{N} P_{\mathrm{mec}}^i \tag{14}$$

$$\text{s.t.} \qquad F_{\mathrm{WF}}^C - F_{\mathrm{WF}}^A < \delta_F \cdot F_{\mathrm{WF}}^A \tag{15}$$

$$0 \le P_{\mathrm{ref}}^i \le P_{\mathrm{WT}}^{\max} \tag{16}$$

where F_{WF}^C and F_{WF}^A are the fatigue load level of the WF using strategy C and strategy A, respectively; δ_F is the tolerant increase ratio of the fatigue load level, which is chosen as 0.05 in this paper.

D. Optimization Method

The problems for WF dispatch strategies B and C are nonlinear and non-convex, therefore the Particle Swarm Optimization (PSO) algorithm is chosen to get the solution [38]. In PSO, the velocity and position are updated based on the equation given below:

$$v_{id}^{k+1} = v_{id}^k + c_1 r_1 \left(p_{id}^k - x_{id}^k\right) + c_2 r_2 \left(p_{gd}^k - x_{id}^k\right) \tag{17}$$

$$x_{id}^{k+1} = v_{id}^{k+1} + x_{id}^k \tag{18}$$

where v_{id}^k and x_{id}^k are the velocity and positions of i-particle in *d*-dimension and the *k*-iteration, c_1 and c_2 are acceleration coefficient, r_1 and r_2 are random numbers in (0, 1) interval, p_{id}^k is

the individual optimum's positions of *i*-particle in *d*-dimension, p_{gd}^k is the global optimum's positions in *d*-dimension.

In order to improve the performance of standard PSO, a linearly time-varying acceleration constant is applied as suggested in [38]. It modifies the velocity updating method with a high cognitive constant (c_1) and low social constant (c_2), and gradually decreases c_1 and increases c_2 to search the entire search space rather than to converge towards a local minimum:

$$c_1(k) = (c_{1,\min} - c_{1,\max})\, k/k_{\max} + c_{1,\max} \tag{19}$$

$$c_2(k) = (c_{2,\max} - c_{2,\min})\, k/k_{\max} + c_{2,\min} \tag{20}$$

where *k* is the iteration number and $k_{\max}$ is the maximum iteration number.

Another modification is to make the maximum velocity $v_{\max}$ decrease with the increase of iterations. This can ensure that the PSO algorithm has good initial explorations and a proper convergence in the final stage [39]. The maximum velocity at each iteration is controlled as:

$$v_{\max}^k = \begin{cases} v_{\max}^{\text{start}} - \frac{k}{\frac{1}{3}k_{\max}}\left(v_{\max}^{\text{start}} - v_{\max}^{\text{end}}\right); & k \le \frac{1}{3}k_{\max} \\ v_{\max}^{\text{end}}; & \text{otherwise} \end{cases}, \tag{21}$$

$$\text{with} \qquad v_{\max}^{\text{start}} = (x_{\max} - x_{\min})/N_s \tag{22}$$

$$v_{\max}^{\text{end}} = (x_{\max} - x_{\min})/N_e \tag{23}$$

where $x_{\min}$ and $x_{\max}$ are the lower and upper bound limits on control variables, and N_s and N_e are constants which control the starting and ending maximum velocity of the particles. In this paper, $k_{\max}$ is chosen as 50 and N_s and N_e are chosen as 20 and 75 separately.

The convergence speed of the Modified PSO (MPSO) can be improved by properly handling the constraints. In this paper, a penalty factor method [40] is adopted to handle the constraints, where the objective function for Strategy C will be defined by:

$$\max_{P_{\text{ref}}^i}\left\{\sum_{i=1}^{N} P_{\text{mec}}^i - \lambda\cdot\left(F_{\text{WF}}^C - F_{\text{WF}}^A - \delta_F\cdot F_{\text{WF}}^A\right)\right\}. \tag{24}$$

The other constraints should be satisfied in the WT control level, which is the inner loop of the optimization problem. The weighting parameter λ should be tuned by testing under each operation condition. The flowchart of the MPSO algorithm for solving Strategy B and Strategy C is shown in Fig. 6.

The fitness function receives the particle position values P_{ref}^i from the MPSO main function, and the WF input wind speed v_0 and WF input turbulence intensity I_0, then calculates the fitness values using the WT model, the wind velocity model and the turbulence intensity model described in Section II. The fitness values are fed back to the initial particle position setting function and the fitness evaluation function to evaluate the particles.

IV. Case Study

A WF which has 5 rows with 5 turbines each row is used to test the strategies. The WF is laid out in a quadrate pattern with a distance of 7 rotor diameters between the turbines, which is shown in Fig. 7. The 5 MW NERL WT is used as the reference WT, whose parameters are shown in Table I [25]:

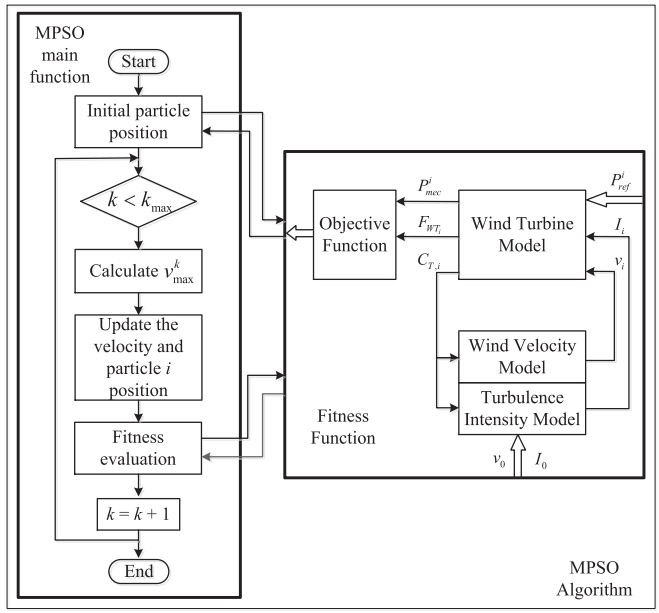

Fig. 6. The flowchart of the MPSO algorithm.

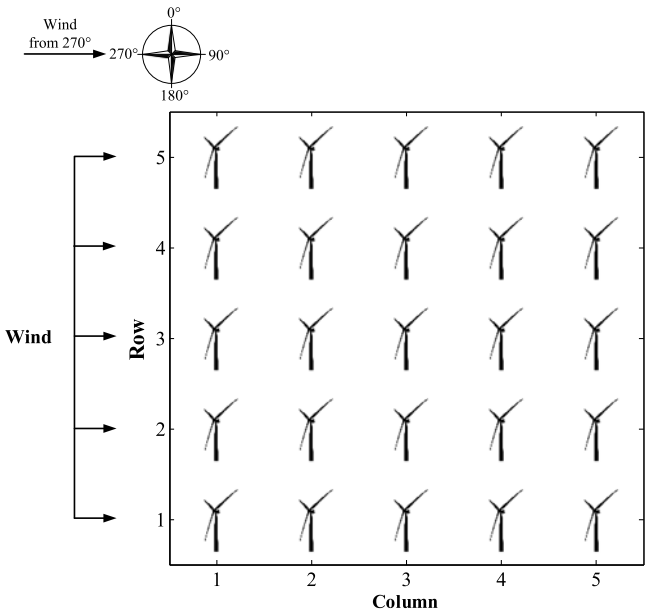

Fig. 7. The wind farm layout.

A. *Scenario I: v = 10 m/s, Wind Direction = 270°,* Ti = 0.1

In this scenario, the incoming wind of the WF has a velocity of 10 m/s, a direction of 270° and a turbulence intensity level of 0.1. The captured wind energy and the fatigue load level of the WF are calculated for each dispatch strategy with these inputs. Because the DEL in 10 mins is adopted in the WT fatigue load lookup table, the captured energy is defined as the accumulated captured power in 10 mins. In order to get better results, the optimizations for strategy B and strategy C are performed

TABLE I
NERL 5 MW WIND TURBINE PARAMETERS

Parameter	5 MW NERL WT
Cut-in, Rated, Cut-out Wind Speed	3 m/s, 11.4 m/s, 25 m/s
Rotor, Hub Diameter	126 m, 3m
Rated Power	5 MW
Cut-In, Rated Rotor Speed	6.9 rpm, 12.1 rpm

TABLE II
THE CAPTURED POWER AND FATIGUE LOAD LEVEL USING DIFFERENT DISPATCH STRATEGIES

	Captured energy in 10 min (MWh)	WF fatigue load level
Strategy A	8.312	1.059
Strategy B	8.8959	1.1973
Strategy C	8.8137	1.1196
Strategy B–Strategy A	0.5839	0.1383
Strategy C–Strategy A	0.5017	0.0606

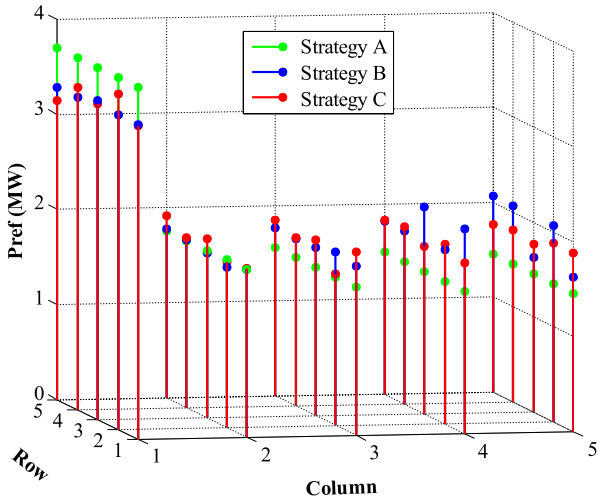

Fig. 8. The average power reference settings of each WT in 10 mins simulation using different dispatch strategies.

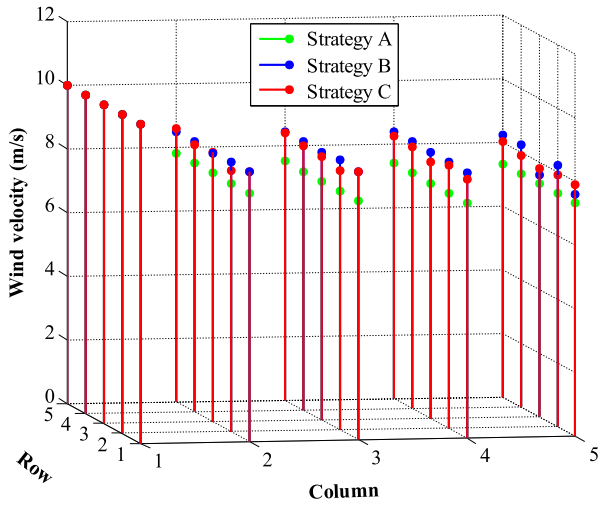

Fig. 9. The average wind velocity at each WT in 10 mins simulation using different dispatch strategies.

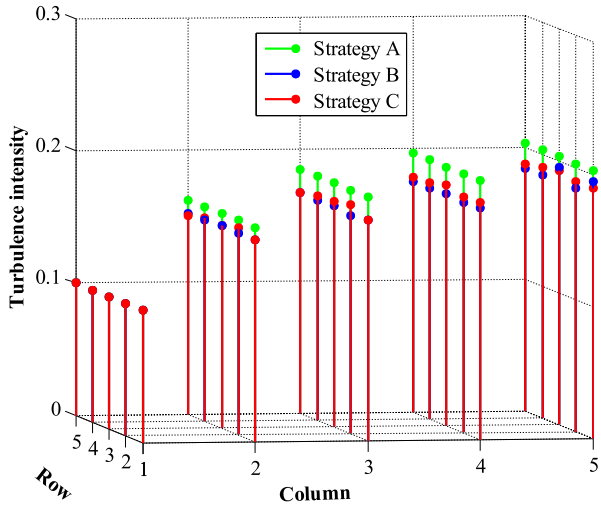

Fig. 10. The turbulence intensity at each WT in 10 mins using different dispatch strategies.

50 times using MPSO and the best result is chosen as the solution. The swarm size of the MPSO is set as 50 and the maximum iteration time set as 60. An Intel(R) Core(TM) i7-4800MQ CPU @ 2.70 GHz processor with 8 GB RAM is used for simulation. The proposed strategy, Strategy C, takes 625 seconds for one time simulation. Using parallel computing with 4 cores, the total computing time of Strategy C for 50 times simulation is 8929 seconds. The results are listed in Table II.

It can be seen that the captured energy using Strategy B is the highest between these three strategies. However, the WF fatigue load level using Strategy B is also the highest. Comparing to Strategy B, the captured energy increase using Strategy C is not as high as Strategy B, but the WF fatigue load level using Strategy C is less than that using Strategy B and is within a certain range of deviation from the fatigue load level using Strategy A. The increase of the captured wind energy from Strategy A to Strategy B and from Strategy A to Strategy C are also listed in the table. The captured energy increase using Strategy B is 0.5839 MWh, which accounts for 7.02% of the captured energy using Strategy A. However, the fatigue load level increases 13.1% with respect to Strategy A, which is also significant. Therefore, Strategy C is better than Strategy B considering the fatigue load level.

More information may be revealed by investigating the distribution of the WT variables within the WF. The power reference setting, the wind velocity, the turbulence intensity, the turbulence and the fatigue load of each WT are the variables with interest and their values using different dispatch strategies are captured and plotted in Figs. 8–12. The power reference settings and the wind velocity are averaged within 10 mins. It can be observed that the power reference of each WT in the first column is reduced using Strategy B and Strategy C (see Fig. 8), but the captured power and wind velocity at downwind WTs are increased (see Figs. 8 and 9). Thus, the power captured at downwind WTs are increased and the total captured power in the WF is raised up.

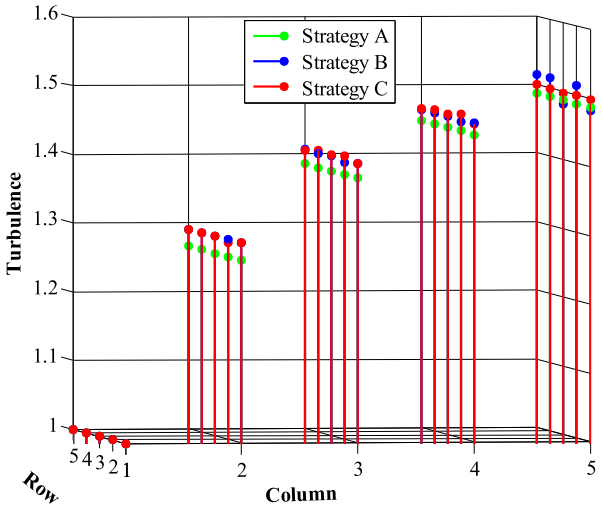

Fig. 11. The turbulence at each WT in 10 mins using different dispatch strategies.

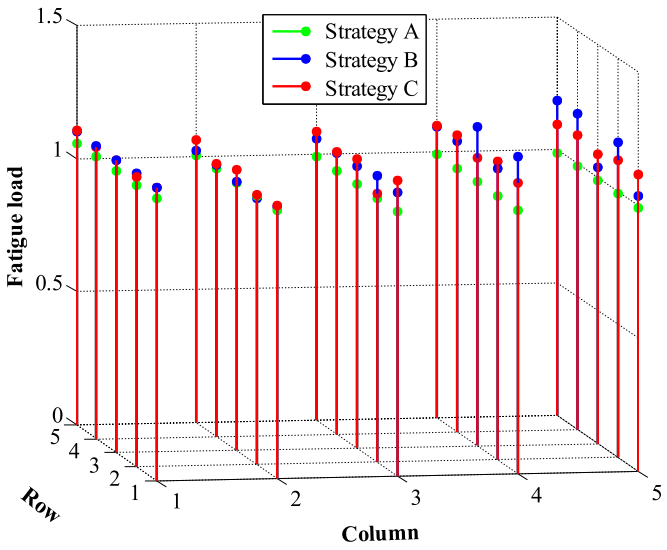

Fig. 12. The fatigue load of each WT in 10 mins using different dispatch strategies.

It also can be observed that the turbulence intensity at the downwind WTs is reduced using Strategy B and Strategy C (see Fig. 10), comparing with Strategy A. However, the turbulence, which equals to the turbulence intensity times wind velocity, is increased (see Fig. 11). Meanwhile, the fatigue load using Strategy B and Strategy C is higher than that using Strategy A (see Fig. 12), and the WF fatigue load level is the highest using Strategy B. Therefore, derating more power at upwind WTs can reduce the wind velocity deficit at downwind WTs and bring more power to the WF, however it will increase the turbulence thus increase the fatigue load at downwind WTs.

B. Scenario II: Wind Direction $= 270°$, Ti $= 0.1$, *Change* v

In this scenario, the effects of different wind velocities to the performance of these strategies are investigated. The wind velocity range is 5 m/s to 14 m/s because beyond this range,

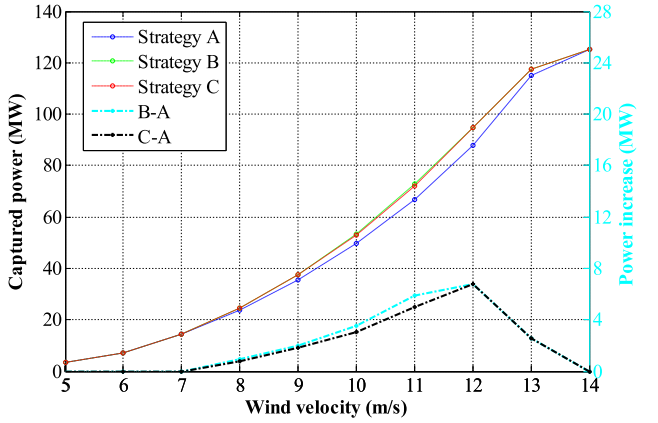

Fig. 13. The average captured power of the WF in 10 mins using different dispatch strategies with the change of wind velocity.

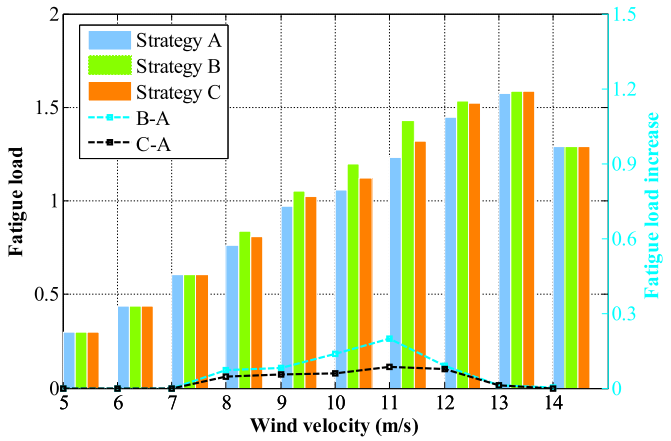

Fig. 14. The fatigue load level of the WF in 10 mins using different dispatch strategies with the change of wind velocity.

most WTs are still not cut-in or working at rated power, thus there is no freedom to change the power reference settings to these WTs. The average captured power of the WF in 10 mins using these dispatch strategies, and the power increase from Strategy A to Strategy B and from Strategy A to Strategy C are shown in Fig. 13. It can be seen that Strategy B can bring the highest captured power at each wind velocity. In addition, the captured power using Strategy C is lower than that of Strategy B, but is higher than the captured power using Strategy A.

The WF fatigue load level using different dispatch strategies and the increase from Strategy A to Strategy B and from Strategy A to Strategy C are shown in Fig. 14. Comparing with Strategy B, Strategy C reduces the WF fatigue load level when the wind velocity is between 7 m/s and 12 m/s. However, the WF fatigue load level at other wind velocity is not reduced, because the constraint (15) is not violated at these wind velocities. When constraint (15) is violated between 7 m/s and 12 m/s, the fatigue load level is reduced to stay within a certain range from the fatigue load level of Strategy A, however the captured power is also reduced comparing to Strategy B. Thus, it can be concluded that the purpose of maximizing the captured power violate with the purpose to reduce the fatigue load level. The proposed strat-

TABLE III
THE SENSITIVITY ANALYSIS OF THE CAPTURED POWER AND THE WF FATIGUE LOAD LEVEL AGAINST THE WIND VELOCITY

Wind velocity (m/s)	Captured power (MW)	WF fatigue load level
9.99	51.7987	1.1204
10	52.8823	1.1196
10.01	52.9897	1.1355

TABLE IV
THE SENSITIVITY ANALYSIS OF THE CAPTURED POWER AND THE WF FATIGUE LOAD LEVEL AGAINST THE WIND DIRECTION

Wind direction (degree)	Captured power (MW)	WF fatigue load level
269	52.8785	1.1186
270	52.8823	1.1196
271	52.8586	1.1192

egy, Strategy C, is a compromise which maximizes the captured power while keep the fatigue load level within a certain range from that of the traditional control strategy.

C. Sensitivity Analysis

The sensitivity analysis of the captured power and the WF fatigue load level against the wind velocity and wind direction is performed around the wind condition where $v = 10$ m/s, wind direction $= 270°$ and $Ti = 0.1$. The optimized power settings under this wind condition, which is calculated using the proposed strategy, is used under the deviated wind conditions. The results are shown in Tables III and IV.

It can be seen from the tables that the captured power and the WF fatigue load level is more sensitive to the change of wind velocity than to the change of wind direction. That is because the change of wind direction causes less change to the wind velocity. Meanwhile, the wind velocity change will affect the available power of each WT and change the thrust coefficient, Ct, which affects the added turbulence that changes the fatigue load. In order to reduce the effects of the sensitivity to wind velocity, smaller wind velocity interval should be set for generating the lookup table used for WF control.

V. CONCLUSION

An optimized active power dispatch strategy is developed in this paper to maximize the total captured power in WFs while maintain the DEL of the shaft and the tower of each WT within a certain range from the values using traditional strategy. The strategy considers the wind deficit model, the added turbulence model, the WT detailed model that includes the WT derating control strategy and a fatigue load model, which is represented by a lookup table. Two traditional strategies are compared with the proposed strategy and the results show the effectiveness of the proposed strategy. The proposed strategy can be used in WF energy management systems or wind power dispatch centers. This strategy uses the power reference as the control variable of WTs as the conventional WT control strategy, thus the implementation of this optimized strategy does not require any modification on the WT controller. Further development of this dispatch strategy will be to be combined with an optimized reactive power dispatch strategy, in order to minimizing the total active power loss and increase the output power.

REFERENCES

[1] "Global Wind Energy Council," Global Wind Report - Annual Market Update 2015, 2015. [Online]. Available: http://www.gwec.net/publications

[2] T. Knudsen, T. Bak, and M. Svenstrup, "Survey of wind farm control—Power and fatigue optimization," *Wind Energy*, vol. 18, pp. 1333–1351, 2014.

[3] F. González-Longatt, P. Wall, and V. Terzija, "Wake effect in wind farm performance: Steady-state and dynamic behavior," *Renew. Energy*, vol. 39, no. 1, pp. 329–338, Mar. 2012.

[4] J. Serrano Gonzalez, M. Burgos Payan, and J. Riquelme Santos, "Optimal control of wind turbines for minimizing overall wake effect losses in offshore wind farms," in *Proc. IEEE EUROCON*, 2013, pp. 1129–1134.

[5] P. M. Gebraad, "Data-driven wind plant control," Delft Univ. Technol., Delft, The Netherlands, 2014.

[6] S. K. Kanev and F. J. Savenije, "Active wake control: Loads trends," ECN, 2015.

[7] M. Churchfield, J. Michalakes, P. Spalart, and P. Moriarty, "Evaluating techniques for redirecting turbine wake using SOWFA," *Renewable Energy*, vol. 70, pp. 211–218, 2013.

[8] P. M. O. Gebraad and J. W. van Wingerden, "Maximum power-point tracking control for wind farms: Maximum power-point tracking control for wind farms," *Wind Energy*, vol. 18, no. 3, pp. 429–447, Mar. 2015.

[9] J. R. Marden, S. D. Ruben, and L. Y. Pao, "A model-free approach to wind farm control using game theoretic methods," *IEEE Trans. Control Syst. Technol.*, vol. 21, no. 4, pp. 1207–1214, Jul. 2013.

[10] J. P. Goit and J. Meyers, "Analysis of turbulent flow properties and energy fluxes in optimally controlled wind-farm boundary layers," *J. Phys., Conf. Ser.*, vol. 524, Jun. 2014, Art. no. 012178.

[11] T. Horvat, V. Spudić, and M. Baotić, "Quasi-stationary optimal control for wind farm with closely spaced turbines," in *Proc. 35th Int. Convention MIPRO*, 2012, pp. 829–834.

[12] J. Lee, E. Son, B. Hwang, and S. Lee, "Blade pitch angle control for aerodynamic performance optimization of a wind farm," *Renewable Energy*, vol. 54, pp. 124–130, Jun. 2013.

[13] A. Behnood, H. Gharavi, B. Vahidi, and G. H. Riahy, "Optimal output power of not properly designed wind farms, considering wake effects," *Int. J. Elect. Power Energy Syst.*, vol. 63, pp. 44–50, Dec. 2014.

[14] J. Serrano González, M. Burgos Payán, J. Riquelme Santos, and Á. G. González Rodríguez, "Maximizing the overall production of wind farms by setting the individual operating point of wind turbines," *Renew. Energy*, vol. 80, pp. 219–229, Aug. 2015.

[15] Y. Guo *et al.* "An approximate wind turbine control system model for wind farm power control," *IEEE Trans. Sustain. Energy*, vol. 4, no. 1, pp. 262–274, Jan. 2013.

[16] H. Sutherland, "On the fatigue analysis of wind turbines," SAND99-0089, Sandia Nat. Labs, Albuquerque, NM, USA, 1999.

[17] V. Spudić, M. Jelavić, and M. Baotić, "Wind turbine power references in coordinated control of wind farms," *Autom. Control Meas. Electron. Comput. Commun.*, vol. 52, no. 2, pp. 82–94, 2011.

[18] M. Soleimanzadeh, "Wind farms: Modeling and control," Ph.D. dissertation, Automation and Control, Dept. Electron. Syst., Aalborg Univ., Aalborg, Denmark, 2011.

[19] V. Spudic, M. Baotic, M. Jelavic, and N. Peric, "Hierarchical wind farm control for power/load optimization," in *Proc. Conf. Sci. Making Torque Wind*, 2010, pp. 681–692.

[20] B. Biegel, "Distributed control of wind farm," Master's Thesis, Automation and Control, Dept. Electron. Syst., Aalborg Univ., Aalborg, Denmark, 2011.

[21] V. Spudic, M. Baotic, and N. Peric, "Wind farm load reduction via parametric programming based controller design," in *Proc. 18th IFAC World Congr.*, 2011, pp. 1704–1709.

[22] T. A. Clevenhult and F. Himmelman, "Added turbulence and optimal power distribution in large off-shore wind farms," Master's Thesis, Dept. Autom. Control, Lund Univ., Lund, Sweden, 2010.

[23] T. N. Jensen, T. Knudsen, and T. Bak, "Fatigue minimising power reference control of a de-rated wind farm," *J. Phys., Conf. Series*, vol. 733, pp. 2–11, 2016.

[24] J. D. Grunnet *et al.*, "Aeolus toolbox for dynamics wind farm model, simulation and control," in *Proc. Eur. Wind Energy Conf. Exhib.*, 2010, pp. 3119–3129.
[25] J. Jonkman *et al.*, "Definition of a 5-mw reference wind turbine for offshore system development," NREL, Golden, CO, USA, Tech. Rep. NREL/TP-500-38060, Feb. 2009.
[26] M. Mirzaei *et al.*, "Turbine control strategies for wind farm power optimization," in *Proc. Amer. Control Conf.*, 2015, pp. 1709–1714.
[27] M. Mirzaei *et al.*, "Model based active power control of a wind turbine," in *Proc. Amer. Control Conf.*, 2014, pp. 5037–5042.
[28] G. Hayman, NWTC Design Codes (MCrunch). [Online]. Available: https://nwtc.nrel.gov/MCrunch Accessed on: Mar. 2016.
[29] B. Zhang *et al.*, "A wind farm active power dispatch strategy for fatigue load reduction," in *Proc. 2016 Amer. Control Conf.*, Boston, MA, USA, 2016, pp. 5879–5884.
[30] P. S. Veers, "Three-dimensional wind simulation," Tech. Rep. SAND-88-0152C; CONF-890102-9, Sandia National Labs., Albuquerque, NM, USA, Jan. 1988.
[31] P. Hou *et al.*, "Optimized placement of wind turbines in large-scale offshore wind farm using particle swarm optimization algorithm," *IEEE Trans. Sustain. Energy*, vol. 6, no. 4, pp. 1272–1282, Oct. 2015.
[32] N. O. Jensen, "A note on wind generator interaction," Tech. Rep. Risø M-2411, Risø, Roskilde, Denmark, 1983.
[33] P. Beaucage *et al.*, "Overview of six commercial and research wake models for large offshore wind farms," in *Proc. Eur. Wind Energy Assoc.*, 2012.
[34] S. T. Frandsen, "Turbulence and turbulence-generated structural loading in wind turbine clusters," Risø Nat. Lab., Roskilde, Denmark, 2007.
[35] P. Hou *et al.*, "Optimised power dispatch strategy for offshore wind farms," *IET Renew. Power Gener.*, vol. 10, no. 3, pp. 399–409, 2016.
[36] B. Zhang *et al.*, "Wind farm active power dispatch for output power maximizing based on a wind turbine control strategy for load minimizing," in *Proc. Int. Conf. Sustain. Mobility Appl., Renewables Technol.*, Kuwait, 2015, pp. 1–6.
[37] B. Zhang *et al.*, "Coordinated power dispatch of a PMSG based wind farm for output power maximizing considering the wake effect and losses," in *Proc. 2016 Power Energy Soc. General Meeting*, Boston, MA, USA, 2016, pp. 1–5.
[38] P. N. Suganthan, "Particle swarm optimiser with neighbourhood operator," in *Proc. Congr. Evol. Comput.*, 1999, pp. 1958–1962.
[39] M. Clerc and J. Kennedy, "The particle swarm - explosion, stability, and convergence in a multidimensional complex space," *IEEE Trans. Evol. Comput.*, vol. 6, no. 1, pp. 58–73, Feb. 2002.
[40] M. A. Abido, "Optimal power flow using tabu search algorithm," *Elect. Power Compon. Syst.*, vol. 30, no. 5, pp. 469–483, 2002.

Baohua Zhang (S'14) received the B.Eng. degree in thermal energy and power engineering from China University of Mining and Technology, Xuzhou, China, in 2009, and the M.Sc. degree in electrical engineering from Shenyang University of Technology, Shenyang, China, in 2013. He is currently working toward the Ph.D. degree in the Department of Energy Technology, Aalborg University, Aalborg, Denmark.

His research interests include wind farm control and energy management systems.

Mohsen Soltani (S'05–M'08–SM'16) received the M.Sc. degree in electrical engineering from Sharif University of Technology, Tehran, Iran, and the Ph.D. degree in electrical and electronic engineering from Aalborg University, Aalborg, Denmark, in 2004 and 2008, respectively.

He was a Visiting Researcher at Eindhoven University of Technology, Eindhoven, The Netherlands, in 2007. He fulfilled a Postdoctoral and an Assistant Professor Program with Aalborg University in 2008–2012. In 2010, he was a Visiting Scholar at Stanford University, Stanford, CA, USA. He is currently an Associate Professor with the Department of Energy Technology, Aalborg University. His research interests include modeling, control, estimation, fault detection, and their applications to electromechanical and energy conversion systems, wind turbines, and wind farms.

Weihao Hu (S'06–M'13–SM'15) received the B.Eng. and M.Sc. degrees from Xi'an Jiaotong University, Xi'an, China, in 2004 and 2007, respectively, both in electrical engineering, and the Ph.D. degree from Aalborg University, Aalborg, Denmark, in 2012.

He is currently an Associate Professor in the Department of Energy Technology, Aalborg University, Denmark. He is the Vice Program Leader of Wind Power System Research Program in the Department of Energy Technology, Aalborg University. His research interests include wind power generation and intelligent energy systems. He has participated in several national and international research projects and he has more than 90 publications in his technical field.

He is currently serving as a Secretary and Treasurer of Power and Energy Society Chapter, IEEE Denmark Section.

Peng Hou (S'14) received the B.Eng. degree from Hebei University of Technology, Tianjin, China, in 2008 and the M.Sc. degree from Chalmers University of Technology, Gothenburg, Sweden, in 2010, both in electrical engineering. He is currently working toward the Ph.D. degree in the Department of Energy Technology, Aalborg University, Aalborg, Denmark.

His research interests include wind farm layout design and optimization algorithm applications.

Qi Huang (S'99–M'03–SM'09) received the B.S. degree in electrical engineering from Fuzhou University, Fuzhou, China, in 1996, the M.S. degree from Tsinghua University, Beijing, China, in 1999, and the Ph.D. degree from Arizona State University, Tempe, AZ, USA, in 2003.

He is currently a Professor at the University of Electronics Science and Technology of China, the Executive Dean of School of Energy Science and Engineering, UESTC, and the Director of Sichuan State Provincial Lab of Power System Wide-area Measurement and Control. His current research and academic interests include power system instrumentation, power system wide area measurement and control, power system informatics and energy blockchain.

Zhe Chen (M'95–SM'98) received the B.Eng. and M.Sc. degrees from Northeast China Institute of Electric Power Engineering, Jilin, China, and the Ph.D. degree from University of Durham, Durham, U.K.

He is a Full Professor with the Department of Energy Technology, Aalborg University, Denmark. He is the Leader of Wind Power System Research Program in the Department of Energy Technology, Aalborg University and the Danish Principle Investigator for Wind Energy of Sino-Danish Centre for Education and Research.

His research areas include power systems, power electronics and electric machines; and his main current research interests are wind energy and modern power systems. He has led many research projects and has more than 400 publications in his technical field.

Dr Chen is an Editor of the IEEE TRANSACTIONS ON POWER SYSTEMS, an Associate Editor of the IEEE TRANSACTIONS ON POWER ELECTRONICS, a Fellow of the Institution of Engineering and Technology, London, U.K., and a Chartered Engineer in the U.K.